

A Study of Production and Decays of Ω_c^0 Baryons at *BABAR*

The *BABAR* Collaboration

November 14, 2018

Abstract

Production and decay of Ω_c^0 baryons is studied with $\sim 230 \text{ fb}^{-1}$ of data recorded with the *BABAR* detector at the PEP-II e^+e^- asymmetric-energy storage ring at SLAC. The Ω_c^0 is reconstructed through its decays into $\Omega^-\pi^+$, $\Omega^-\pi^+\pi^-\pi^+$, and $\Xi^-K^-\pi^+\pi^+$ final states.

The invariant mass spectra are presented and the signal yields are extracted. Ratios of branching fractions are measured relative to the $\Omega_c^0 \rightarrow \Omega^-\pi^+$ mode

$$\frac{\mathcal{B}(\Omega_c^0 \rightarrow \Xi^-K^-\pi^+\pi^+)}{\mathcal{B}(\Omega_c^0 \rightarrow \Omega^-\pi^+)} = 0.31 \pm 0.15(\text{stat.}) \pm 0.04(\text{syst.}),$$
$$\frac{\mathcal{B}(\Omega_c^0 \rightarrow \Omega^-\pi^+\pi^-\pi^+)}{\mathcal{B}(\Omega_c^0 \rightarrow \Omega^-\pi^+)} < 0.30 \quad (90\% \text{CL}).$$

The momentum spectrum (not corrected for efficiency) of Ω_c^0 baryons is extracted from decays into $\Omega^-\pi^+$, establishing the first observation of Ω_c^0 production from B decays.

Contributed to the XXIInd International Symposium on Lepton and Photon Interactions at High Energies, 6/30 — 7/5/2005, Uppsala, Sweden

Stanford Linear Accelerator Center, Stanford University, Stanford, CA 94309

Work supported in part by Department of Energy contract DE-AC03-76SF00515.

The BABAR Collaboration,

B. Aubert, R. Barate, D. Boutigny, F. Couderc, Y. Karyotakis, J. P. Lees, V. Poireau, V. Tisserand,
A. Zghiche

Laboratoire de Physique des Particules, F-74941 Annecy-le-Vieux, France

E. Grauges

IFAE, Universitat Autònoma de Barcelona, E-08193 Bellaterra, Barcelona, Spain

A. Palano, M. Pappagallo, A. Pompili

Università di Bari, Dipartimento di Fisica and INFN, I-70126 Bari, Italy

J. C. Chen, N. D. Qi, G. Rong, P. Wang, Y. S. Zhu

Institute of High Energy Physics, Beijing 100039, China

G. Eigen, I. Ofte, B. Stugu

University of Bergen, Institute of Physics, N-5007 Bergen, Norway

G. S. Abrams, M. Battaglia, A. B. Breon, D. N. Brown, J. Button-Shafer, R. N. Cahn, E. Charles,
C. T. Day, M. S. Gill, A. V. Gritsan, Y. Groysman, R. G. Jacobsen, R. W. Kadel, J. Kadyk, L. T. Kerth,
Yu. G. Kolomensky, G. Kukartsev, G. Lynch, L. M. Mir, P. J. Oddone, T. J. Orimoto, M. Pripstein,
N. A. Roe, M. T. Ronan, W. A. Wenzel

Lawrence Berkeley National Laboratory and University of California, Berkeley, California 94720, USA

M. Barrett, K. E. Ford, T. J. Harrison, A. J. Hart, C. M. Hawkes, S. E. Morgan, A. T. Watson

University of Birmingham, Birmingham, B15 2TT, United Kingdom

M. Fritsch, K. Goetzen, T. Held, H. Koch, B. Lewandowski, M. Pelizaeus, K. Peters, T. Schroeder,
M. Steinke

Ruhr Universität Bochum, Institut für Experimentalphysik 1, D-44780 Bochum, Germany

J. T. Boyd, J. P. Burke, N. Chevalier, W. N. Cottingham

University of Bristol, Bristol BS8 1TL, United Kingdom

T. Cuhadar-Donszelmann, B. G. Fulsom, C. Hearty, N. S. Knecht, T. S. Mattison, J. A. McKenna

University of British Columbia, Vancouver, British Columbia, Canada V6T 1Z1

A. Khan, P. Kyberd, M. Saleem, L. Teodorescu

Brunel University, Uxbridge, Middlesex UB8 3PH, United Kingdom

A. E. Blinov, V. E. Blinov, A. D. Bukin, V. P. Druzhinin, V. B. Golubev, E. A. Kravchenko,
A. P. Onuchin, S. I. Serebnyakov, Yu. I. Skovpen, E. P. Solodov, A. N. Yushkov

Budker Institute of Nuclear Physics, Novosibirsk 630090, Russia

D. Best, M. Bondioli, M. Bruinsma, M. Chao, S. Curry, I. Eschrich, D. Kirkby, A. J. Lankford, P. Lund,
M. Mandelkern, R. K. Mommsen, W. Roethel, D. P. Stoker

University of California at Irvine, Irvine, California 92697, USA

C. Buchanan, B. L. Hartfiel, A. J. R. Weinstein

University of California at Los Angeles, Los Angeles, California 90024, USA

S. D. Foulkes, J. W. Gary, O. Long, B. C. Shen, K. Wang, L. Zhang
University of California at Riverside, Riverside, California 92521, USA

D. del Re, H. K. Hadavand, E. J. Hill, D. B. MacFarlane, H. P. Paar, S. Rahatlou, V. Sharma
University of California at San Diego, La Jolla, California 92093, USA

J. W. Berryhill, C. Campagnari, A. Cunha, B. Dahmes, T. M. Hong, M. A. Mazur, J. D. Richman,
W. Verkerke
University of California at Santa Barbara, Santa Barbara, California 93106, USA

T. W. Beck, A. M. Eisner, C. J. Flacco, C. A. Heusch, J. Kroseberg, W. S. Lockman, G. Nesom, T. Schalk,
B. A. Schumm, A. Seiden, P. Spradlin, D. C. Williams, M. G. Wilson
University of California at Santa Cruz, Institute for Particle Physics, Santa Cruz, California 95064, USA

J. Albert, E. Chen, G. P. Dubois-Felsmann, A. Dvoretzki, D. G. Hitlin, I. Narsky, T. Piatenko,
F. C. Porter, A. Ryd, A. Samuel
California Institute of Technology, Pasadena, California 91125, USA

R. Andreassen, S. Jayatilleke, G. Mancinelli, B. T. Meadows, M. D. Sokoloff
University of Cincinnati, Cincinnati, Ohio 45221, USA

F. Blanc, P. Bloom, S. Chen, W. T. Ford, J. F. Hirschauer, A. Kreisel, U. Nauenberg, A. Olivas,
P. Rankin, W. O. Ruddick, J. G. Smith, K. A. Ulmer, S. R. Wagner, J. Zhang
University of Colorado, Boulder, Colorado 80309, USA

A. Chen, E. A. Eckhart, J. L. Harton, A. Soffer, W. H. Toki, R. J. Wilson, Q. Zeng
Colorado State University, Fort Collins, Colorado 80523, USA

D. Altenburg, E. Feltresi, A. Hauke, B. Spaan
Universität Dortmund, Institut für Physik, D-44221 Dortmund, Germany

T. Brandt, J. Brose, M. Dickopp, V. Klose, H. M. Lacker, R. Nogowski, S. Otto, A. Petzold, G. Schott,
J. Schubert, K. R. Schubert, R. Schwierz, J. E. Sundermann
Technische Universität Dresden, Institut für Kern- und Teilchenphysik, D-01062 Dresden, Germany

D. Bernard, G. R. Bonneaud, P. Grenier, S. Schrenk, Ch. Thiebaut, G. Vasileiadis, M. Verderi
Ecole Polytechnique, LLR, F-91128 Palaiseau, France

D. J. Bard, P. J. Clark, W. Gradl, F. Muheim, S. Playfer, Y. Xie
University of Edinburgh, Edinburgh EH9 3JZ, United Kingdom

M. Andreotti, V. Azzolini, D. Bettoni, C. Bozzi, R. Calabrese, G. Cibinetto, E. Luppi, M. Negrini,
L. Piemontese
Università di Ferrara, Dipartimento di Fisica and INFN, I-44100 Ferrara, Italy

F. Anulli, R. Baldini-Ferrolì, A. Calcaterra, R. de Sangro, G. Finocchiaro, P. Patteri, I. M. Peruzzi,¹
M. Piccolo, A. Zallo
Laboratori Nazionali di Frascati dell'INFN, I-00044 Frascati, Italy

¹Also with Università di Perugia, Dipartimento di Fisica, Perugia, Italy

A. Buzzo, R. Capra, R. Contri, M. Lo Vetere, M. Macri, M. R. Monge, S. Passaggio, C. Patrignani,
E. Robutti, A. Santroni, S. Tosi

Università di Genova, Dipartimento di Fisica and INFN, I-16146 Genova, Italy

G. Brandenburg, K. S. Chaisanguanthum, M. Morii, E. Won, J. Wu

Harvard University, Cambridge, Massachusetts 02138, USA

R. S. Dubitzky, U. Langenegger, J. Marks, S. Schenk, U. Uwer

Universität Heidelberg, Physikalisches Institut, Philosophenweg 12, D-69120 Heidelberg, Germany

W. Bhimji, D. A. Bowerman, P. D. Dauncey, U. Egede, R. L. Flack, J. R. Gaillard, G. W. Morton,
J. A. Nash, M. B. Nikolich, G. P. Taylor, W. P. Vazquez

Imperial College London, London, SW7 2AZ, United Kingdom

X. Chai, M. J. Charles, W. F. Mader, U. Mallik, A. K. Mohapatra, V. Ziegler

University of Iowa, Iowa City, Iowa 52242, USA

J. Cochran, H. B. Crawley, V. Eyges, W. T. Meyer, S. Prell, E. I. Rosenberg, A. E. Rubin, J. Yi

Iowa State University, Ames, Iowa 50011-3160, USA

N. Arnaud, M. Davier, X. Giroux, G. Grosdidier, A. Höcker, F. Le Diberder, V. Lepeltier, A. M. Lutz,
A. Oyanguren, T. C. Petersen, M. Pierini, S. Plaszczynski, S. Rodier, P. Roudeau, M. H. Schune,
A. Stocchi, G. Wormser

Laboratoire de l'Accélérateur Linéaire, F-91898 Orsay, France

C. H. Cheng, D. J. Lange, M. C. Simani, D. M. Wright

Lawrence Livermore National Laboratory, Livermore, California 94550, USA

A. J. Bevan, C. A. Chavez, I. J. Forster, J. R. Fry, E. Gabathuler, R. Gamet, K. A. George,
D. E. Hutchcroft, R. J. Parry, D. J. Payne, K. C. Schofield, C. Touramanis

University of Liverpool, Liverpool L69 7ZE, United Kingdom

C. M. Cormack, F. Di Lodovico, W. Menges, R. Sacco

Queen Mary, University of London, E1 4NS, United Kingdom

C. L. Brown, G. Cowan, H. U. Flaecher, M. G. Green, D. A. Hopkins, P. S. Jackson, T. R. McMahon,
S. Ricciardi, F. Salvatore

University of London, Royal Holloway and Bedford New College, Egham, Surrey TW20 0EX, United Kingdom

D. Brown, C. L. Davis

University of Louisville, Louisville, Kentucky 40292, USA

J. Allison, N. R. Barlow, R. J. Barlow, C. L. Edgar, M. C. Hodgkinson, M. P. Kelly, G. D. Lafferty,
M. T. Naisbit, J. C. Williams

University of Manchester, Manchester M13 9PL, United Kingdom

C. Chen, W. D. Hulsbergen, A. Jawahery, D. Kovalskyi, C. K. Lae, D. A. Roberts, G. Simi

University of Maryland, College Park, Maryland 20742, USA

G. Blaylock, C. Dallapiccola, S. S. Hertzbach, R. Kofler, V. B. Koptchev, X. Li, T. B. Moore, S. Saremi,
H. Staengle, S. Willocq

University of Massachusetts, Amherst, Massachusetts 01003, USA

R. Cowan, K. Koeneke, G. Sciolla, S. J. Sekula, M. Spitznagel, F. Taylor, R. K. Yamamoto
*Massachusetts Institute of Technology, Laboratory for Nuclear Science, Cambridge, Massachusetts 02139,
USA*

H. Kim, P. M. Patel, S. H. Robertson
McGill University, Montréal, Quebec, Canada H3A 2T8

A. Lazzaro, V. Lombardo, F. Palombo
Università di Milano, Dipartimento di Fisica and INFN, I-20133 Milano, Italy

J. M. Bauer, L. Cremaldi, V. Eschenburg, R. Godang, R. Kroeger, J. Reidy, D. A. Sanders, D. J. Summers,
H. W. Zhao

University of Mississippi, University, Mississippi 38677, USA

S. Brunet, D. Côté, P. Taras, B. Viaud
Université de Montréal, Laboratoire René J. A. Lévesque, Montréal, Quebec, Canada H3C 3J7

H. Nicholson
Mount Holyoke College, South Hadley, Massachusetts 01075, USA

N. Cavallo,² G. De Nardo, F. Fabozzi,² C. Gatto, L. Lista, D. Monorchio, P. Paolucci, D. Piccolo,
C. Sciacca

Università di Napoli Federico II, Dipartimento di Scienze Fisiche and INFN, I-80126, Napoli, Italy

M. Baak, H. Bulten, G. Raven, H. L. Snoek, L. Wilden
*NIKHEF, National Institute for Nuclear Physics and High Energy Physics, NL-1009 DB Amsterdam, The
Netherlands*

C. P. Jessop, J. M. LoSecco
University of Notre Dame, Notre Dame, Indiana 46556, USA

T. Allmendinger, G. Benelli, K. K. Gan, K. Honscheid, D. Hufnagel, P. D. Jackson, H. Kagan, R. Kass,
T. Pulliam, A. M. Rahimi, R. Ter-Antonyan, Q. K. Wong

Ohio State University, Columbus, Ohio 43210, USA

J. Brau, R. Frey, O. Igonkina, M. Lu, C. T. Potter, N. B. Sinev, D. Strom, J. Strube, E. Torrence
University of Oregon, Eugene, Oregon 97403, USA

F. Galeazzi, M. Margoni, M. Morandin, M. Posocco, M. Rotondo, F. Simonetto, R. Stroili, C. Voci
Università di Padova, Dipartimento di Fisica and INFN, I-35131 Padova, Italy

M. Benayoun, H. Briand, J. Chauveau, P. David, L. Del Buono, Ch. de la Vaissière, O. Hamon,
M. J. J. John, Ph. Leruste, J. Malclès, J. Ocariz, L. Roos, G. Therin
*Universités Paris VI et VII, Laboratoire de Physique Nucléaire et de Hautes Energies, F-75252 Paris,
France*

²Also with Università della Basilicata, Potenza, Italy

P. K. Behera, L. Gladney, Q. H. Guo, J. Panetta
University of Pennsylvania, Philadelphia, Pennsylvania 19104, USA

M. Biasini, R. Covarelli, S. Pacetti, M. Pioppi
Università di Perugia, Dipartimento di Fisica and INFN, I-06100 Perugia, Italy

C. Angelini, G. Batignani, S. Bettarini, F. Bucci, G. Calderini, M. Carpinelli, R. Cenci, F. Forti,
M. A. Giorgi, A. Lusiani, G. Marchiori, M. Morganti, N. Neri, E. Paoloni, M. Rama, G. Rizzo, J. Walsh
Università di Pisa, Dipartimento di Fisica, Scuola Normale Superiore and INFN, I-56127 Pisa, Italy

M. Haire, D. Judd, D. E. Wagoner
Prairie View A&M University, Prairie View, Texas 77446, USA

J. Biesiada, N. Danielson, P. Elmer, Y. P. Lau, C. Lu, J. Olsen, A. J. S. Smith, A. V. Telnov
Princeton University, Princeton, New Jersey 08544, USA

F. Bellini, G. Cavoto, A. D'Orazio, E. Di Marco, R. Faccini, F. Ferrarotto, F. Ferroni, M. Gaspero, L. Li
Gioi, M. A. Mazzoni, S. Morganti, G. Piredda, F. Polci, F. Safai Tehrani, C. Voena
Università di Roma La Sapienza, Dipartimento di Fisica and INFN, I-00185 Roma, Italy

H. Schröder, G. Wagner, R. Waldi
Universität Rostock, D-18051 Rostock, Germany

T. Adye, N. De Groot, B. Franek, G. P. Gopal, E. O. Olaiya, F. F. Wilson
Rutherford Appleton Laboratory, Chilton, Didcot, Oxon, OX11 0QX, United Kingdom

R. Aleksan, S. Emery, A. Gaidot, S. F. Ganzhur, P.-F. Giraud, G. Graziani, G. Hamel de Monchenault,
W. Kozanecki, M. Legendre, G. W. London, B. Mayer, G. Vasseur, Ch. Yèche, M. Zito
DSM/Dapnia, CEA/Saclay, F-91191 Gif-sur-Yvette, France

M. V. Purohit, A. W. Weidemann, J. R. Wilson, F. X. Yumiceva
University of South Carolina, Columbia, South Carolina 29208, USA

T. Abe, M. T. Allen, D. Aston, N. van Bakel, R. Bartoldus, N. Berger, A. M. Boyarski, O. L. Buchmueller,
R. Claus, J. P. Coleman, M. R. Convery, M. Cristinziani, J. C. Dingfelder, D. Dong, J. Dorfan, D. Dujmic,
W. Dunwoodie, S. Fan, R. C. Field, T. Glanzman, S. J. Gowdy, T. Hadig, V. Halyo, C. Hast, T. Hryn'ova,
W. R. Innes, M. H. Kelsey, P. Kim, M. L. Kocian, D. W. G. S. Leith, J. Libby, S. Luitz, V. Luth,
H. L. Lynch, H. Marsiske, R. Messner, D. R. Muller, C. P. O'Grady, V. E. Ozcan, A. Perazzo, M. Perl,
B. N. Ratcliff, A. Roodman, A. A. Salnikov, R. H. Schindler, J. Schwiening, A. Snyder, J. Stelzer, D. Su,
M. K. Sullivan, K. Suzuki, S. Swain, J. M. Thompson, J. Va'vra, M. Weaver, W. J. Wisniewski,
M. Wittgen, D. H. Wright, A. K. Yarritu, K. Yi, C. C. Young
Stanford Linear Accelerator Center, Stanford, California 94309, USA

P. R. Burchat, A. J. Edwards, S. A. Majewski, B. A. Petersen, C. Roat
Stanford University, Stanford, California 94305-4060, USA

M. Ahmed, S. Ahmed, M. S. Alam, J. A. Ernst, M. A. Saeed, F. R. Wappler, S. B. Zain
State University of New York, Albany, New York 12222, USA

W. Bugg, M. Krishnamurthy, S. M. Spanier
University of Tennessee, Knoxville, Tennessee 37996, USA

R. Eckmann, J. L. Ritchie, A. Satpathy, R. F. Schwitters
University of Texas at Austin, Austin, Texas 78712, USA

J. M. Izen, I. Kitayama, X. C. Lou, S. Ye
University of Texas at Dallas, Richardson, Texas 75083, USA

F. Bianchi, M. Bona, F. Gallo, D. Gamba
Università di Torino, Dipartimento di Fisica Sperimentale and INFN, I-10125 Torino, Italy

M. Bomben, L. Bosisio, C. Cartaro, F. Cossutti, G. Della Ricca, S. Dittongo, S. Grancagnolo, L. Lanceri,
L. Vitale
Università di Trieste, Dipartimento di Fisica and INFN, I-34127 Trieste, Italy

F. Martinez-Vidal
IFIC, Universitat de Valencia-CSIC, E-46071 Valencia, Spain

R. S. Panvini³
Vanderbilt University, Nashville, Tennessee 37235, USA

Sw. Banerjee, B. Bhuyan, C. M. Brown, D. Fortin, K. Hamano, R. Kowalewski, J. M. Roney, R. J. Sobie
University of Victoria, Victoria, British Columbia, Canada V8W 3P6

J. J. Back, P. F. Harrison, T. E. Latham, G. B. Mohanty
Department of Physics, University of Warwick, Coventry CV4 7AL, United Kingdom

H. R. Band, X. Chen, B. Cheng, S. Dasu, M. Datta, A. M. Eichenbaum, K. T. Flood, M. Graham,
J. J. Hollar, J. R. Johnson, P. E. Kutter, H. Li, R. Liu, B. Mellado, A. Mihalyi, Y. Pan, R. Prepost,
P. Tan, J. H. von Wimmersperg-Toeller, S. L. Wu, Z. Yu
University of Wisconsin, Madison, Wisconsin 53706, USA

H. Neal
Yale University, New Haven, Connecticut 06511, USA

³Deceased

1 INTRODUCTION

The Ω_c^0 (*css*) is a ($J^P = \frac{1}{2}^+$)[‡] ground state baryon with a mass of $m_{\Omega_c^0} = (2697.5 \pm 2.6) \text{ MeV}/c^2$ and a lifetime of $\tau_{\Omega_c^0} = (69 \pm 12) \text{ fs}$ [1]. Since the first evidence for Ω_c^0 production and decay in 1984 [2] in the decay mode $\Omega_c^0 \rightarrow \Xi^- K^- \pi^+ \pi^+$, the Ω_c^0 baryon has been seen by a number of different experiments [3–8] in various decay modes, with strong evidence reported in the decays $\Omega_c^0 \rightarrow \Omega^- \pi^+$, $\Omega_c^0 \rightarrow \Xi^- K^- \pi^+ \pi^+$, and $\Omega_c^0 \rightarrow \Sigma^+ K^- K^- \pi^+$. To date, only one 5σ observation has been reported by a single experiment, combining two modes [8]. No observation of a single exclusive Ω_c^0 decay mode at the 5σ level has been reported and only a few of its decay modes have been observed. The measurements of the ratios of branching fractions still have large uncertainties and the production mechanisms of the Ω_c^0 remain largely unexplored.

The large amount of data collected at the B factories allows a more detailed analysis of the properties of the Ω_c^0 . In this paper, a study of the Ω_c^0 through the decay modes⁴ $\Omega^- \pi^+$, $\Omega^- \pi^+ \pi^- \pi^+$, and $\Xi^- K^- \pi^+ \pi^+$ is described.

The invariant mass spectra are presented and the ratios of branching fractions relative to the $\Omega^- \pi^+$ decay mode are calculated. To study the production mechanism, the Ω_c^0 momentum spectrum (not corrected for efficiency) in the e^+e^- rest frame is presented.

2 THE BABAR DETECTOR AND DATASET

The *BABAR* detector operating at the PEP-II e^+e^- asymmetric-energy storage ring at SLAC consists of a tracking system for the detection of charged particles, a detector of internally reflected Cherenkov light (DIRC), an electromagnetic calorimeter (EMC), and an instrumented flux return (IFR). The tracking system, contained in a 1.5-T magnetic field provided by a superconducting solenoidal coil, includes a 5-layer, double-sided silicon vertex tracker (SVT) and a 40-layer drift chamber (DCH). The EMC consists of 6580 CsI(Tl) crystals. Information from the DIRC and the energy loss information from the SVT and the DCH are used for charged particle identification (PID). The IFR is segmented and instrumented with resistive plate chambers. The *BABAR* detector is described in detail elsewhere [9].

This analysis is based on data taken at the $\Upsilon(4S)$ resonance and $\sim 40 \text{ MeV}/c^2$ below, referred to as on-peak and off-peak data, respectively. The integrated luminosity of the data used corresponds to $\sim 225 \text{ fb}^{-1}$ in each of the Ω_c^0 decay modes involving an Ω^- , and $\sim 230 \text{ fb}^{-1}$ in the Ξ^- decay mode.

To minimize the selection bias, all selection criteria are optimized on Monte Carlo simulated event samples at least as large as the data sample. Samples of $e^+e^- \rightarrow q\bar{q}$ ($q \in \{u, d, s, c\}$) events are used to study the background. Monte Carlo samples are used to study the signal properties and to evaluate the selection efficiencies. The Ω_c^0 signal samples are generated with JETSET [10], assuming uniform phase space for the Ω_c^0 decays.

3 EVENT SELECTION

The Ω^- (Ξ^-) is reconstructed in its ΛK^- ($\Lambda \pi^-$) final state. Candidates for Λ decays are reconstructed in their $p\pi^-$ final state. The branching fractions [1] of the intermediate hyperons are $\mathcal{B}(\Omega^- \rightarrow \Lambda K^-) = (67.8 \pm 0.7)\%$, $\mathcal{B}(\Xi^- \rightarrow \Lambda \pi^-) \sim 100\%$, and $\mathcal{B}(\Lambda \rightarrow p\pi^-) = (63.9 \pm 0.5)\%$.

[‡]The quantum numbers have not been measured, but are assigned in accord with the quark model.

⁴Simultaneous treatment of the charge conjugate mode is always implied throughout the note.

3.1 The Hyperon Selection

All hyperons in this analysis (Λ , Ξ^- , and Ω^-) are long-lived particles with a typical decay length of several cm in *BABAR*. Each hyperon is identified by reconstructing its decay vertex, which is required to be clearly displaced from that of the parent particle. In the selection of each of the intermediate hyperons, only candidates with an invariant mass within 3σ of the central value are selected, where σ denotes the invariant mass resolution. These candidates are then subjected to a kinematic fit, constraining the mass of the candidate to its nominal value.

Candidates of Λ baryons are formed from a pair of tracks of opposite charge, where the positively charged track must satisfy the PID requirements for a proton. Each Λ candidate is combined with a π^- (K^-) to form a Ξ^- (Ω^-) candidate. The K^- candidate track from the Ω^- decay must satisfy the PID requirements for kaons.

Candidates for Ω_c^0 decays for each final state are formed by combining the reconstructed Ω^- and Ξ^- baryons with the required number of mesons (π^- , π^+ , or K^-). Throughout this document, mesons that are the direct daughters of the Ω_c^0 candidate are referred to as ‘primary mesons’.

3.2 The Ω_c^0 Candidate Selection

The kinematics of the signal decays and the backgrounds are different for each of the Ω_c^0 decay channels considered in this analysis. The Q -values, which are a measure of the available kinetic energy of the decay products, are 882 MeV, 603 MeV, and 595 MeV for the $\Omega^- \pi^+$, $\Omega^- \pi^+ \pi^- \pi^+$, and $\Xi^- K^- \pi^+ \pi^+$ decay modes, respectively. Therefore, the selection criteria are optimized for each mode separately. Particle identification is required for each of the primary mesons. The selection criteria described below are then applied to the Ω_c^0 candidates in order to suppress backgrounds. In addition, a common minimum p^* of 2.8 GeV/ c is required for candidates used in the measurement of the ratios of branching fractions, where p^* is the Ω_c^0 momentum in the e^+e^- rest frame. This is above the kinematic limit for Ω_c^0 production from B decays ($p^* = 2.02$ GeV/ c).

- $\Omega_c^0 \rightarrow \Omega^- \pi^+$:

The transverse flight length of the Ω^- candidate in the xy -plane calculated with respect to the event vertex is required to exceed 2 mm. The signed⁵ flight length of the Λ , measured from the Ω^- decay point, must exceed 1.5 mm. For the primary pion, a minimum momentum of 200 MeV/ c in the laboratory frame is required. A minimum of 0.1% is required for the χ^2 -probability of the kinematic fit for each intermediate hyperon.

- $\Omega_c^0 \rightarrow \Omega^- \pi^+ \pi^- \pi^+$:

The transverse flight length of the Ω^- candidate in the xy -plane calculated with respect to the event vertex is required to exceed 2.5 mm. The signed flight length of the Λ , measured from the Ω^- decay point, must exceed 2 mm. The vector sum of the momenta of the $\pi^+ \pi^- \pi^+$ system in the lab-frame is required to exceed 650 MeV/ c . A minimum of 0.1% is required for the χ^2 -probability of the kinematic fit for each intermediate hyperon.

- $\Omega_c^0 \rightarrow \Xi^- K^- \pi^+ \pi^+$:

The minimum requirement on the flight length of the Ξ^- is 4.5 mm and the signed flight length of the Λ with respect to the Ξ^- decay vertex is required to be larger than zero. A minimum χ^2 probability of 10^{-4} is required for the kinematic fit of the full decay chain.

⁵The signed flight length is defined as the dot product of the displacement vector ($\vec{r}_\Lambda - \vec{r}_\Omega$) of the Λ and the momentum vector of the Λ , where \vec{r} denotes the 3D position of the vertex.

4 THE INVARIANT MASS SPECTRA

The signal yield for each decay mode is extracted from an unbinned maximum likelihood fit to the invariant mass spectrum of the Ω_c^0 candidates. In the fit, the signal lineshape is described by a sum of three Gaussians with a common mean, and the background is described by a first order ($\Omega^- \pi^+$ mode) or second order (all other modes) polynomial. The widths and relative contributions of each Gaussian are fixed to the values obtained from samples of simulated Ω_c^0 baryons produced in $c\bar{c}$ continuum and decayed in the considered mode. The mean mass, the yield of the signal peak, and the parameters in the polynomial for the description of the background are left free in the fit to the data. In the fit to the $\Omega^- \pi^+ \pi^- \pi^+$ mode, due to the small signal, the mean of the signal lineshape is fixed to the weighted mean⁶ ($\mu = 2694.6 \text{ MeV}/c^2$) obtained from the fits to the other two decay modes.

The invariant mass spectra are displayed in Figures 1(a-c) for the $\Omega^- \pi^+$, $\Omega^- \pi^+ \pi^- \pi^+$, and $\Xi^- K^- \pi^+ \pi^+$ modes. The results of the fits to the data, the selection efficiencies⁷, and the χ^2

⁶This is not necessarily the true mass of the Ω_c^0 baryon. No studies of systematic biases due to energy loss corrections of the decay products or due to the uncertainties on the energy and momentum scale are carried out.

⁷All selection efficiencies quoted are for Ω_c^0 decays with $p^* > 2.8 \text{ GeV}/c^2$.

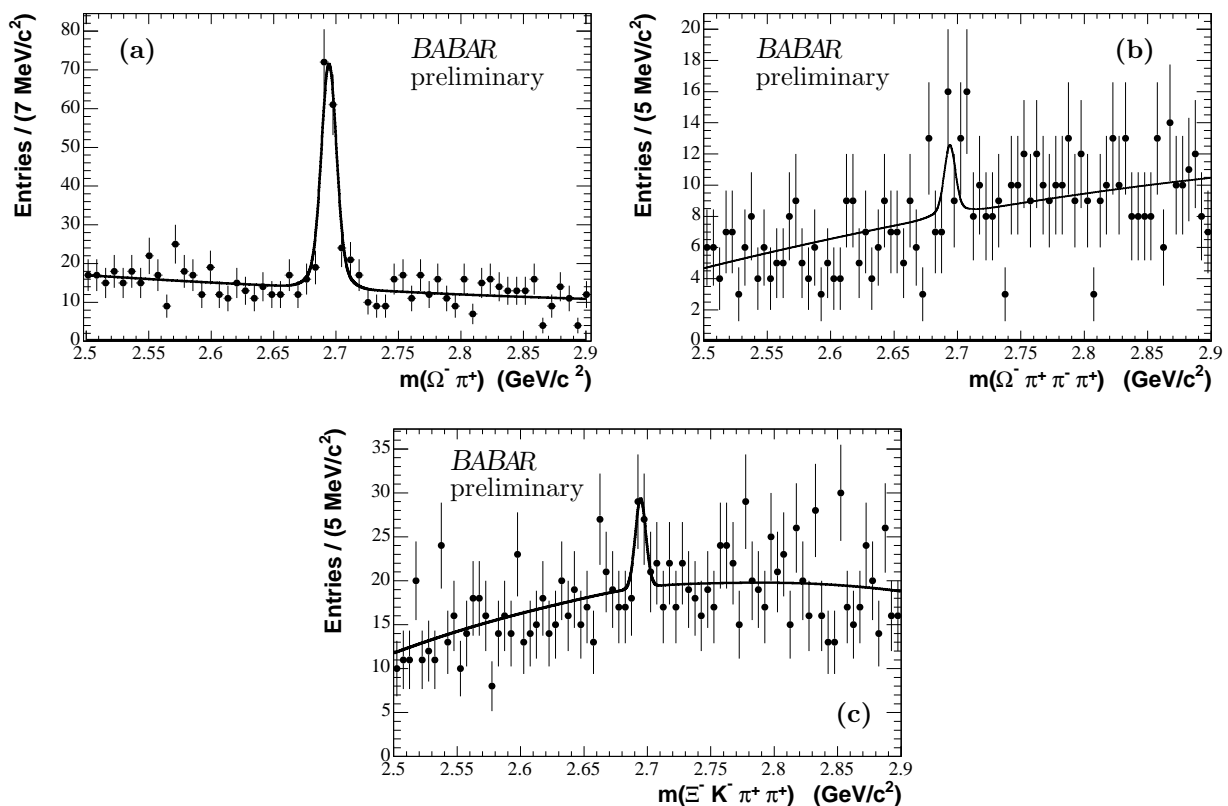


Figure 1: Invariant mass spectra for Ω_c^0 decays into (a) $\Omega^- \pi^+$, (b) $\Omega^- \pi^+ \pi^- \pi^+$, and (c) $\Xi^- K^- \pi^+ \pi^+$ final states with $p^* > 2.8 \text{ GeV}/c$. The dots are the data. The binning is chosen according to the Half-Width-Half-Maximum of the signal peak obtained from signal Monte Carlo. The result of the fit is overlaid

Table 1: Results from the fits to the invariant mass spectra in data. The yields (not corrected for efficiency) are given for each mode individually, as well as the selection efficiencies. In addition the χ^2 probability for the fit, calculated in the mass window $2.6 < m < 2.8 \text{ GeV}/c^2$, and the significance \mathcal{S} of the signal is quoted for the $\Omega^-\pi^+\pi^-\pi^+$ and the $\Xi^-K^-\pi^+\pi^+$ modes.

| Decay Mode | Signal Yield | Efficiency (%) | prob(χ^2) | \mathcal{S} |
|---------------------------|------------------|-----------------|------------------|---------------|
| $\Omega^-\pi^+$ | 138.5 ± 14.8 | 8.35 ± 0.07 | 0.54 | 17.8 |
| $\Omega^-\pi^+\pi^-\pi^+$ | 11.8 ± 7.5 | 4.41 ± 0.09 | 0.73 | 2.4 |
| $\Xi^-K^-\pi^+\pi^+$ | 29.9 ± 13.6 | 5.63 ± 0.10 | 0.85 | 3.4 |

probability for each fit are summarized in Table 1. In addition, the significance \mathcal{S} for the signal, defined as $\sqrt{2\Delta \log \mathcal{L}}$, calculated from the difference in the log-likelihood ($\log \mathcal{L}$) for a fit with and without a signal lineshape, is included.

5 PRODUCTION MECHANISM FOR Ω_c^0 BARYONS

Insight into the production mechanism for Ω_c^0 baryons is obtained from the p^* spectrum. For this study, the $\Omega_c^0 \rightarrow \Omega^-\pi^+$ decay mode, which has the largest signal yield of all modes in this analysis, is used. The signal yield as a function of p^* is measured up to $4.4 \text{ GeV}/c$ in eleven intervals, each $400 \text{ MeV}/c$ wide. For each interval, the $\Omega^-\pi^+$ invariant mass spectrum is fit with the lineshape for the signal fixed to that obtained from the full signal Monte Carlo sample. A polynomial is used to describe the background. No significant variation in the central value of the signal peak is observed as a function of p^* . It is therefore fixed to the common mean for all intervals in the fit.

The measured signal yields obtained from the combined on-peak and off peak data sets can be compared with those from the off-peak data set, displayed in Figures 2(a) and 2(b), respectively. The dots represent the data and the error bars correspond to the statistical uncertainty only. The solid horizontal bars correspond to the predicted spectrum for Ω_c^0 production from $c\bar{c}$ continuum Monte Carlo; the thickness of the bars correspond to the statistical uncertainty. No correction for selection efficiency is applied to either distribution. The corresponding distribution from signal Monte Carlo is normalized such that its integral corresponds to that in data for $p^* > 2.5 \text{ GeV}/c$ in Figure 2(a), and for the full p^* range in Figure 2(b).

A clear two-peak structure is evident in the distribution from the combined on-peak and off-peak data sets. The peak at high p^* is consistent with Ω_c^0 production as predicted from continuum signal Monte Carlo and the off-peak data. The p^* spectra from data and Monte Carlo show good agreement within the experimental uncertainties in this region. The peak in the p^* region below $2.02 \text{ GeV}/c$ provides clear first evidence for Ω_c^0 production from B decays. This interpretation is substantiated by the absence of the corresponding peak in the spectrum extracted from off-peak data only, taken below the $B\bar{B}$ threshold.

6 PHYSICS RESULTS

6.1 Ratios of Branching Fractions

The yields for Ω_c^0 signal events, extracted from the invariant mass spectra in the data and corrected for selection efficiency and acceptance effects. These are extracted from reconstructed signal Monte

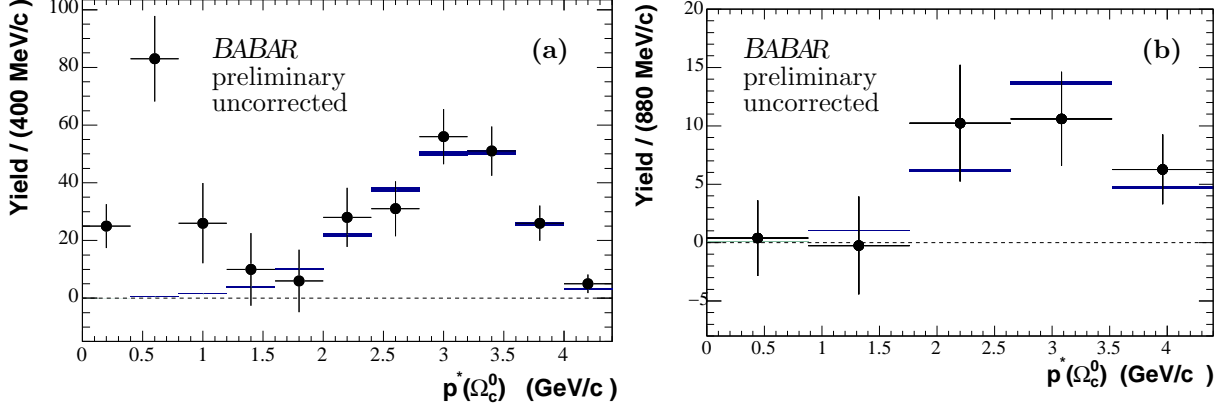


Figure 2: The signal yield as a function of the p^* of Ω_c^0 candidates (a) from the combined on-peak and off-peak data sets and (b) from off-peak data only. The dots are the data and the vertical error bars correspond to the statistical uncertainty only. The solid horizontal bars correspond to the predicted distribution for Ω_c^0 production from $c\bar{c}$ continuum signal Monte Carlo. The thickness of the bars correspond to the statistical uncertainty of the Monte Carlo sample. No correction for selection efficiency is applied to any of the distributions shown. The distributions are normalized to the same area for (a) $p^* > 2.5$ GeV/c and (b) the full range. In (a), clear evidence for Ω_c^0 production from B decays is visible at low p^* . It is absent in off-peak data (b), collected below the $B\bar{B}$ production threshold.

Carlo events that pass the same selection criteria as events in data. The efficiency corrected yields are then used to calculate the ratios of branching fractions relative to the $\Omega_c^0 \rightarrow \Omega^- \pi^+$ mode, yielding

$$\frac{\mathcal{B}(\Omega_c^0 \rightarrow \Omega^- \pi^+ \pi^- \pi^+)}{\mathcal{B}(\Omega_c^0 \rightarrow \Omega^- \pi^+)} = 0.16 \pm 0.10(\text{stat.}) \pm 0.03(\text{syst.}),$$

$$\frac{\mathcal{B}(\Omega_c^0 \rightarrow \Xi^- K^- \pi^+ \pi^+)}{\mathcal{B}(\Omega_c^0 \rightarrow \Omega^- \pi^+)} = 0.31 \pm 0.15(\text{stat.}) \pm 0.04(\text{syst.}).$$

The individual contributions to the systematic uncertainties are discussed in detail in Section 6.2.

6.2 Systematic Studies

Although the decay topologies are slightly different in the various decay modes, the systematic uncertainties on the hyperon selection efficiencies largely cancel in the ratios of branching fractions. The following sources of systematic uncertainties are considered in the measurement of the ratios of branching fractions and summarized in Table 2.

- Monte Carlo Simulation:

The statistical uncertainty on the selection efficiencies is taken into account in the systematic uncertainty.

In multi-body decay modes, the decay can occur via intermediate resonances. Therefore, signal Monte Carlo samples containing the $\Xi^*(1530)^0 K^- \pi^+$, the $\Xi^- K^{*0} \pi^+$, and the $\Xi^*(1530)^0 K^{*0}$ decay modes are generated. The difference in selection efficiencies relative to the uniform-phase-space sample is included as an uncertainty on the selection efficiency. For the $\Omega^- \pi^+ \pi^- \pi^+$

mode, the systematic uncertainty associated with intermediate resonances is assumed to be the same as that for the topologically similar mode $\Xi^- K^- \pi^+ \pi^+$.

The p^* spectrum of the Ω_c^0 in data and Monte Carlo is slightly (but not significantly) different. The effect on the selection efficiency is calculated and a systematic uncertainty accounting for the difference is assigned. This contribution is correlated for the decay mode in the numerator and in the denominator and is treated accordingly in the calculation of the systematic uncertainty on the ratio of branching fractions.

- Extraction of the Signal Yield:

In the fit to the invariant mass spectra, the description of the background shape is varied for the purpose of estimating the systematic uncertainty. In addition, the width of the widest Gaussian in the description of the signal shape is varied by a factor of two, and the fit range is varied from $2.6 < m < 2.8 \text{ GeV}/c^2$ to $2.4 < m < 3.0 \text{ GeV}/c^2$. The observed variations in the signal yield are added as a systematic uncertainty.

- Particle Identification and Tracking:

The number of primary mesons is different for some of the modes. A systematic uncertainty of 1% is added for each additional primary pion, estimated from the uncertainty on the efficiency of the pion identification. A systematic uncertainty of 1% is assigned to account for different kaon identification algorithms used for the primary and non-primary kaons.

In order to account for the difference in tracking efficiency in data and Monte Carlo, a correction of 0.25% with a systematic uncertainty of 1.4% is applied per track. In the ratio of branching fractions this amounts to a 0.5% correction to the selection efficiency with a systematic uncertainty of 2.8%.

- Branching Fraction:

The Ω^- is identified in its decay to ΛK^- , which has a branching fraction of $(67.8 \pm 0.7)\%$. This uncertainty in the branching fraction is added to the systematic uncertainty for the ratio involving the Ξ^- only. The uncertainty in the Λ branching fraction to $p\pi^-$ cancels in the ratio of branching fractions for all modes.

Table 2: Systematic uncertainties considered in the measurement of the ratios of branching fractions. The individual contributions are given, and added in quadrature to determine the total systematic uncertainty. Dashes indicate sources that are assumed to cancel in the ratio of branching fractions.

| | $\frac{\mathcal{B}(\Omega^- \pi^+ \pi^- \pi^+)}{\mathcal{B}(\Omega^- \pi^+)}$ | $\frac{\mathcal{B}(\Xi^- K^- \pi^+ \pi^+)}{\mathcal{B}(\Omega^- \pi^+)}$ |
|-------------------------------|-------------------------------------------------------------------------------|--------------------------------------------------------------------------|
| Monte Carlo Statistics | 0.004 | 0.006 |
| p^* Reweighting | 0.001 | 0.004 |
| Resonance Structure | 0.003 | 0.005 |
| Extraction of Signal Yield | 0.028 | 0.032 |
| Particle ID & Tracking | 0.006 | 0.011 |
| Ω^- Branching Fraction | -- | 0.003 |
| Multiple Candidates | 0.002 | 0.004 |
| Total Systematic Uncertainty | 0.03 | 0.04 |

- Multiple Candidates:

A possible source of background comes from the presence of multiple Ω_c^0 candidates in an event, which share one or more tracks. Predominantly, the same hyperon combines with one or more primary tracks to form such multiple candidates. In general, these candidates are distributed over a large mass range. However, in cases where these candidates share tracks, their masses might be correlated, which could lead to a pile-up of candidates in the signal region. The mass distribution of Ω_c^0 in events with multiple candidates is studied in data as well as in Monte Carlo signal samples. We select events in which one of the candidates falls inside a ± 3 HWHM mass window around the nominal peak position. In data, two, four, and four events with such multiple candidates are observed in the $\Omega^- \pi^+$, $\Omega^- \pi^+ \pi^- \pi^+$, and $\Xi^- K^- \pi^+ \pi^+$, respectively, where the second candidate also lies in the signal region defined above. From studies of these candidates in a larger mass window, these multiple candidates are observed to be evenly distributed in mass for all modes. Therefore, they form part of the background when the mass spectra are fit with a polynomial. This indicates that there is no statistically significant peaking under the signal peak in data.

The relative sizes of the peaks from incorrectly reconstructed multiple candidates and true signal candidates in Monte Carlo are 0.2%, 1.2% and 1.3% in the $\Omega^- \pi^+$, $\Omega^- \pi^+ \pi^- \pi^+$, and $\Xi^- K^- \pi^+ \pi^+$ mode, respectively. This fraction is assigned as a systematic uncertainty.

- Other Sources of Peaking Background:

Possible sources of peaking backgrounds are studied with continuum Monte Carlo samples. The number of peaking background events observed is consistent with zero and therefore no systematic uncertainty is assigned.

The individual sources of systematic uncertainties are added in quadrature. The total uncertainty on each ratio is given in Table 2.

6.3 Limit Calculation for the $\Omega_c^0 \rightarrow \Omega^- \pi^+ \pi^- \pi^+$ Mode

No significant excess of signal events over the background is observed in the $\Omega^- \pi^+ \pi^- \pi^+$ mode. Therefore, a limit at the 90% confidence level (CL) on the ratio of branching fractions is calculated. The limit is obtained from a Monte Carlo calculation for the individual modes, using the measured yields and the statistical and systematic uncertainties as inputs. All uncertainties are assumed to be Gaussian. Integrating the positive part of the distribution of ratios of branching fractions obtained from these Monte Carlo experiments, an upper limit at the 90% confidence level of

$$\frac{\mathcal{B}(\Omega_c^0 \rightarrow \Omega^- \pi^+ \pi^- \pi^+)}{\mathcal{B}(\Omega_c^0 \rightarrow \Omega^- \pi^+)} < 0.30 \quad (90\% \text{CL})$$

is obtained.

6.4 Cross-checks

Cross-checks for the measurements of the ratios of branching fractions are performed to verify the stability of the result.

- Charge asymmetry:

To obtain the main result, no distinction is made between decays of the Ω_c^0 and the anti-baryon $\overline{\Omega}_c^0$. However, the selection efficiencies might be different due to differences in the interaction in material of particles and anti-particles. Particle and anti-particle candidates are selected and studied separately. The observed difference in efficiency-corrected yields for mode and anti-mode is largest in the Ω_c^0 decay into $\Xi^- K^- \pi^+ \pi^+$, with a difference of 1.6σ . All ratios of branching fractions are found to be consistent within the statistical uncertainties.

- Choice of the p^* range:

The main results for the ratios of branching fractions are obtained for a minimum p^* of $2.8 \text{ GeV}/c$. The ratios of branching fractions, however, are expected to be independent of that choice. As a cross-check, these ratios are recalculated, requiring a p^* in the range $2.6 \text{ GeV}/c < p^* < 3.2 \text{ GeV}/c$ and $p^* > 3.2 \text{ GeV}/c$. All results are found to be consistent within statistical uncertainties.

7 SUMMARY

Data recorded with the *BABAR* detector are analyzed to study Ω_c^0 production and decays. The Ω_c^0 is reconstructed through its decays into $\Omega^- \pi^+$ and $\Omega^- \pi^+ \pi^- \pi^+$ (using 225 fb^{-1} of data), and into $\Xi^- K^- \pi^+ \pi^+$ (using 230 fb^{-1}).

Based on the momentum spectrum of the Ω_c^0 in the e^+e^- rest frame in the full data set and in off-peak data only, the first observation of Ω_c^0 production from B decays is reported.

In the $\Omega^- \pi^+$ decay mode, the Ω_c^0 is observed with a statistical significance of over 17σ . This constitutes the first observation of the Ω_c^0 baryon above the 5σ level.

From the observed signal yields, corrected for efficiency and acceptance, the ratios of branching fractions relative to $\Omega_c^0 \rightarrow \Omega^- \pi^+$ are measured to be

$$\frac{\mathcal{B}(\Omega_c^0 \rightarrow \Omega^- \pi^+ \pi^- \pi^+)}{\mathcal{B}(\Omega_c^0 \rightarrow \Omega^- \pi^+)} = 0.16 \pm 0.10(\text{stat.}) \pm 0.03(\text{syst.}),$$

$$\frac{\mathcal{B}(\Omega_c^0 \rightarrow \Xi^- K^- \pi^+ \pi^+)}{\mathcal{B}(\Omega_c^0 \rightarrow \Omega^- \pi^+)} = 0.31 \pm 0.15(\text{stat.}) \pm 0.04(\text{sys.}),$$

where the first uncertainty is statistical and the second is systematic. Due to the limited statistical significance for the decay mode $\Omega_c^0 \rightarrow \Omega^- \pi^+ \pi^- \pi^+$, an upper limit on the ratio of branching fractions,

$$\frac{\mathcal{B}(\Omega_c^0 \rightarrow \Omega^- \pi^+ \pi^- \pi^+)}{\mathcal{B}(\Omega_c^0 \rightarrow \Omega^- \pi^+)} < 0.30 \quad (90\% \text{CL}),$$

at the 90% confidence level is set. All results mark a considerable improvement, both in statistical and systematic uncertainties, over the current world averages [1].

8 ACKNOWLEDGMENTS

We are grateful for the extraordinary contributions of our PEP-II colleagues in achieving the excellent luminosity and machine conditions that have made this work possible. The success of this project also relies critically on the expertise and dedication of the computing organizations

that support *BABAR*. The collaborating institutions wish to thank SLAC for its support and the kind hospitality extended to them. This work is supported by the US Department of Energy and National Science Foundation, the Natural Sciences and Engineering Research Council (Canada), Institute of High Energy Physics (China), the Commissariat à l’Energie Atomique and Institut National de Physique Nucléaire et de Physique des Particules (France), the Bundesministerium für Bildung und Forschung and Deutsche Forschungsgemeinschaft (Germany), the Istituto Nazionale di Fisica Nucleare (Italy), the Foundation for Fundamental Research on Matter (The Netherlands), the Research Council of Norway, the Ministry of Science and Technology of the Russian Federation, and the Particle Physics and Astronomy Research Council (United Kingdom). Individuals have received support from CONACyT (Mexico), the A. P. Sloan Foundation, the Research Corporation, and the Alexander von Humboldt Foundation.

References

- [1] S. Eidelman *et al.* [Particle Data Group], Phys. Lett. **B 592**, 1 (2004).
- [2] S. F. Biagi *et al.* [WA62 Collaboration], Z. Phys. C **28**, 175 (1985).
- [3] H. Albrecht *et al.* [ARGUS Collaboration], Phys. Lett. B **288**, 367 (1992).
- [4] P. L. Frabetti *et al.* [E687 Collaboration], Phys. Lett. B **300**, 190 (1993).
- [5] P. L. Frabetti *et al.* [E687 Collaboration], Phys. Lett. B **338**, 106 (1994).
- [6] S. Ahmed *et al.* [CLEO Collaboration], Int. J. Mod. Phys. A **16S1B**, 505 (2001).
- [7] M. I. Adamovich *et al.* [WA89 Collaboration], Phys. Lett. B **358**, 151 (1995).
- [8] J. M. Link *et al.* [FOCUS Collaboration], Phys. Lett. B **561**, 41 (2003).
- [9] B. Aubert *et al.* [*BABAR* Collaboration], Nucl. Instrum. Methods **A479**, 1 (2002).
- [10] T. Sjostrand, P. Eden, C. Friberg, L. Lonnblad, G. Miu, S. Mrenna and E. Norrbin, “High-energy-physics event generation with PYTHIA 6.1,” Comput. Phys. Commun. **135**, 238 (2001).